Electrical properties of M-type barium hexaferrites ($BaFe_{12}ZnMnO_{19}$)

Cite as: AIP Conference Proceedings **2251**, 040043 (2020); https://doi.org/10.1063/5.0015695
Published Online: 18 August 2020

A. Doyan, Susilawati, M. Taufik, and Wahyudi

Electrical Properties of M-Type Barium Hexaferrites ($BaFe_{12}ZnMnO_{19}$)

A. Doyan*), Susilawati, M. Taufik, and Wahyudi

Physics Education, FKIP, University of Mataram, Lombok, West Nusa Tenggara, Indonesia.

*)Corresponding author: aris_doyan@unram.ac.id

Abstract. The synthesis of barium hexaferrite M-type with ($BaFe_{12}ZnMnO_{19}$) doped Zn-Mn ion can be applicated as an absorbent of the microwave by the co-precipitation technique. This study to tracing the influence of doping ion was synthesis varied at concentration doping (x = 0.0, 0.6 and 1.0) and temperature maturation 80, 600, and 800 °C on properties of the electrical sample. The samples were characterized by analysis using Network Vector Analyzer (VNA). The result from VNA gets data of conductivity of electrical values at range 8.0 to 15.0 GHz. It is showed that the sample is a semiconductor (5.8×10^{-4} - 1.27×10^{-1} S/cm). The value of permittivity real and imaginary showed that increased with increasing concentration doping and frequency.

INTRODUCTION

The technique of un-detection of an object by the radar rests on two aspects: (1) The object is designed with the angle of the radar absorbing structure (RAS), so that the reflection of electromagnetic waves cannot be recaptured by the receiver, (2) The body of the plane is coated by a wave absorber material radar absorbing materials (RAM) as Barium M-hexaferrite $BaFe_{12}O_{19}$ [1]. A material can absorb radar when interacting with the electric field of the wave, so many magnetic materials are developed. Materials that have the ability to absorb radar is barium M-hexaferrite (BaM) $BaFe_{12}O_{19}$ [2], due to the high magnetocrystalline anisotropy properties, it is necessary to fabricate the properties of materials such as conductivity, coercivity, saturation magnetization, remanence magnetization, and curie temperature to suit the needs by doping Fe ions with other elements such as Co, Zn, Ni, Mn, Ti, and others up to a certain amount. Supplementation is not expected to cause structural changes in the base material considering the dimensions of the doping and doping materials are almost the same [3].

Research is developing rapidly with various methods to obtain barium M-hexaferrite (BaM) in nanosize because particle size largely determines the magnetic characteristics of BaM. The most widely used methods are sol-gel, gas crystallization, ball milling, coprecipitation, aerosols, hydrothermal precipitation, and mechanical integration. Coprecipitation is one method of synthesis of inorganic compounds based on the deposition of more than one material substance mix when more than a saturation point [4].

METHODS

The method used in this research is the true experimental method. The ingredients base for this study is $BaCO_3$, $MnCl_2$, $FeCl_3.6H_2O$, and $ZnCl_2$ (PA) in powder form with a purity of 99.99%. Preparation of barium ferrite ($BaFe_{12-2x}Zn_x\ Mn_xO_{19}$) substitution, using mole fraction x = 0.0, 0.6, and 1.0 using the co-precipitation method. Samples in the form of deposited material were filtered with a paper filter to a neutral pH (seven), washed by pure water, then dried at 80 °C using an oven. Furthermore, the grinding process so as to obtain brown powder and calcined with various temperatures 400, 600, and 800 °C respectively as long as 4 hours [5]. The electrical properties were identified through characterization using VNA (Vector Network Analyzer).

International Conference on Electromagnetism, Rock Magnetism and Magnetic Material (ICE-R3M) 2019
AIP Conf. Proc. 2251, 040043-1–040043-5; https://doi.org/10.1063/5.0015695
Published by AIP Publishing. 978-0-7354-2010-6/$30.00

RESULTS AND DISCUSSION

Identification of electrical properties was done characterization by VNA on $BaFe_{12}O_{19}$ samples with calcination temperatures of 600 °C, $BaFe_{10.8}Zn_{0.6}$-$Mn_{0.6}O_{19}$, and $BaFe_{10}Zn$-MnO_{19} with temperatures of 800 °C in the range frequency 8 - 15 GHz. Data obtained from this test are impedance data in the form of imaginary and real values in the form of Smith charts which are used to obtain conductivity values of samples at various measurement frequencies for each doping mole fraction as shown in Fig. 1.

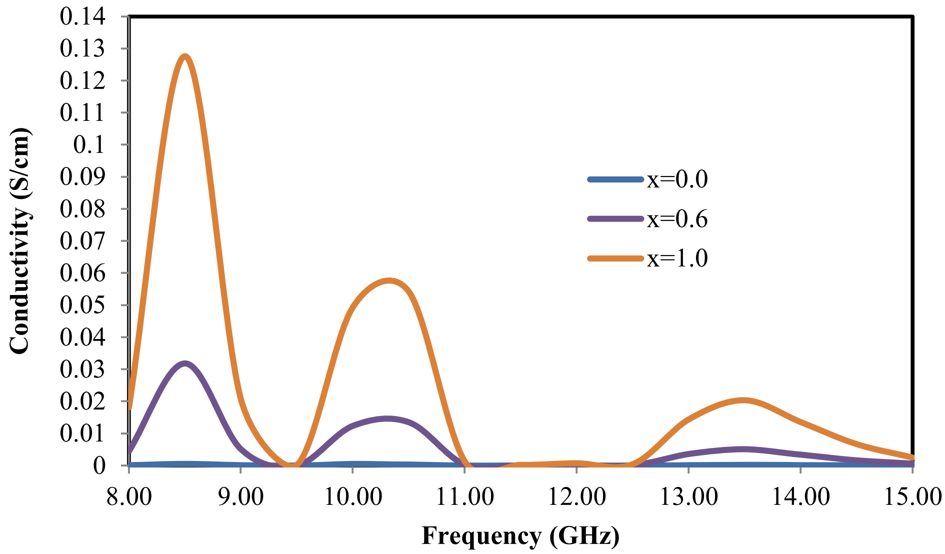

FIGURE 1. Graph conductivity of sample

Figure 1 it can be seen that there are three maximum peaks of conductivity values, at a frequency of 8.5; 10.3 and 13.5 GHz. The conductivity value increases with increasing Zn-Mn doping concentration at all three frequencies. With increasing frequency it is observed that the value of conductivity has decreased, for example in the doped Zn-Mn concentration (x=1) and frequency of 8.5 GHz the conductivity value is 0.13 S/cm and decreases to 0.06 S/cm at a frequency of 10.3 GHz and continues to decrease to 0.025 S/cm at a frequency of 13.5 GHz. To be applied as a microwave-absorbing mineral, the semiconductor material can convert microwave energy into heat energy [6,7]. When microwaves come into contact with minerals that are coated with a microwave absorbent material, an electric field will form on the surface of the absorber. After that, the current to surface simultaneously by the current flows to the absorber, the microwave energy will be transformed into heat energy [8].

Figure 2 and 3 show the value of permittivity and permeability sample in the measurement frequency range (10-15) GHz. Based on Fig. 2 (a), it possibly is seen that the real permittivity (ε') value increases as the increasing frequency at 13 to 15 GHz, while at the frequency of 10-13 GHz the value tends to be constant. The real permittivity value also increases with the increasing amount of Zn-Mn doping concentration. From Fig. 2 (b) it can be seen that the value of imaginary permittivity has decreased at a frequency of 10-11 GHz, and then at a frequency of 11-15 GHz the value tends to be constant. The imaginary permittivity also increases by the increasing amount of Zn-Mn doping concentration. The ε' value was increased together to the transformation from Fe^{3+} to Fe^{2+} ions to be masked so that it causes polarization on the surface of the sample [9,10].

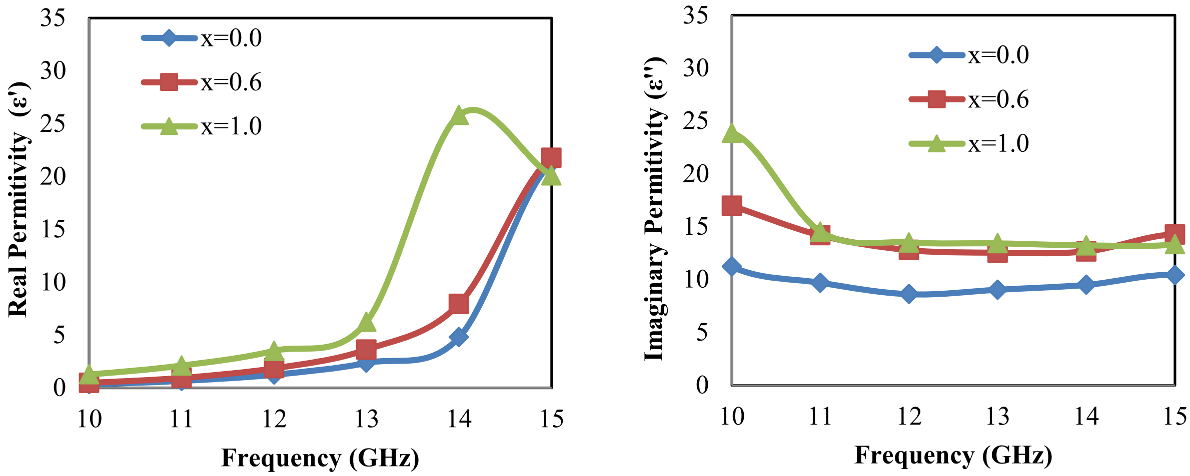

(a) **(b)**

FIGURE 2. Graph of the relationship between frequency versus a). real permittivity and b). Imaginary permittivity of $BaFe_{12-x}Zn_x$-Mn_xO_{19} samples in the frequency range (10-15) GHz.

The sample compared to the real permittivity value of material absorbent barium-hexaferrite, the permittivity value resulting imaginary is lower. The form of an electric field in a sample increased while compared to the ability of a sample to release electrical energy. As a result of supporting the resulting intrinsic dipole moment, a dipole defect is formed in the presence of an electromagnetic field, this causes polarization on the dipole so that the Loss Dielectric tangent (δe) appears.

Figure 3 provides information about the measured sample permeability in the frequency range (10-15) GHz. The resulting permeability (μ) increases with increasing doping mole fraction and frequency. From frequency 13-15 GHz the value of permeability a sharp increased. Imaginary permeability value for doping concentration x = 0 and x = 0.6 has increased, but for concentration x = 1.0 it actually decreases the imaginary permeability value.

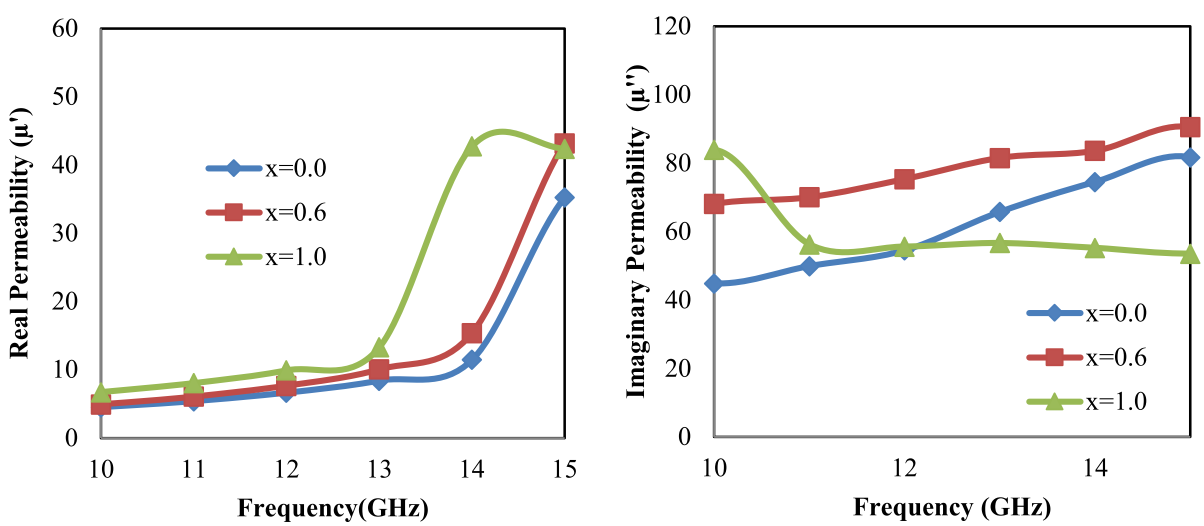

(a) **(b)**

FIGURE 3. Graph of the relationship between frequency versus a). real permeability and b). Imaginary permeability of the $BaFe_{10}Zn$-MnO_{19} sample in the frequency range (10-15) GHz.

If we compare the permittivity and permeability values of the sample as a whole, it appears that the permeability value of the sample is higher than the permittivity value of the sample, this is caused by the doping magnetic moment values of Zn^{2+}, (3μB) and Mn^{2+}, (2.8 μB) higher than the magnetic moment values of Fe^{3+} (5μB) substituted [11]. In research [12] obtained higher permittivity values than the permeability value by using Co-Ti doping because of the magnetic moment Co^{2+}, (3 μB) and Ti^{4+}, (0 μB) is not enough to replace the magnetic moment Fe^{3+}. The permeability and permittivity values of the real part show the amount of microwave energy absorbed by the material and the imaginary value proves the total microwave energy that has been transformed in the form of energy loss [13]. The collaboration of the real value and imaginary value while determines the working frequency area of the material absorb the microwave.

Figure 4(a) showed that relation between dielectric loss tangent (δe) and frequency. The maximum value of dielectric loss tangent (δe) at concentration of doping x = 0.6, it means that the on covering leads to the occurance of lattice distortion thereby increasing electron scattering and resistivity. Fig. 4(b) showed that the value of magnetic loss tangent (δm) decreases with increases frequency. The decrease in δm due to suppression is caused by a decrease in interfacial polarization [14,15]. δm is caused by the displacement in the wall domain, turning domain, wall domain resonance, and natural resonance due to magnetic relaxation in the measurement frequency range [16]. The low value of δm produced indicates the ability of magnetic fields in the sample material is higher when converting to the ability of the sample to release magnetic energy [17].

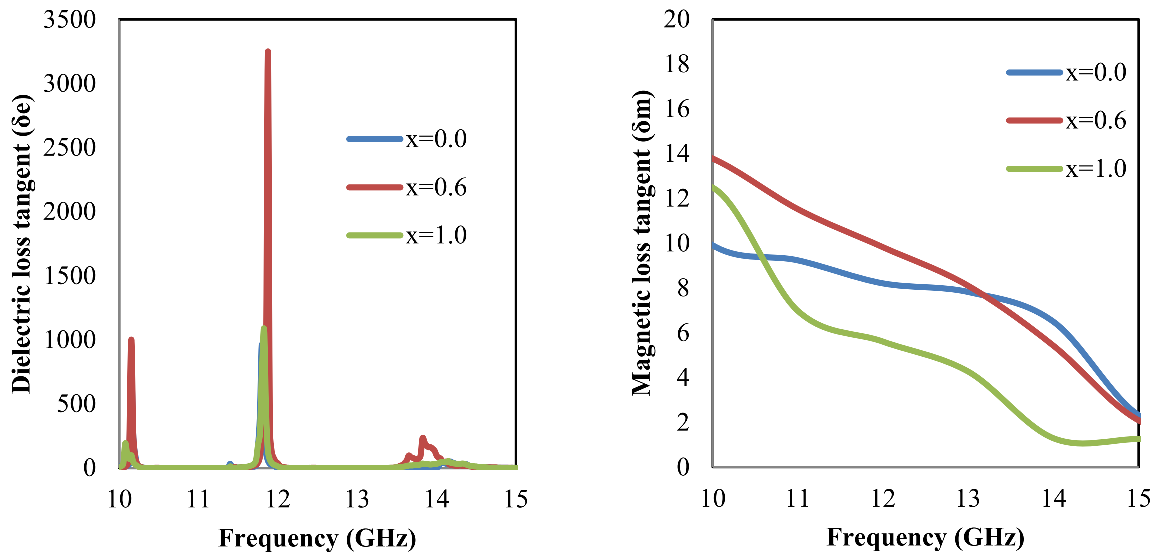

(a) **(b)**

FIGURE 4. Graph of the relationship between a). Dielectric Loss tangent and b). Magnetic Loss tangent of, $BaFe_{10}Zn$-MnO_{19} samples in the frequency range (10-15) GHz.

CONCLUSION

The $BaFe_{12-2x}Zn_x Mn_xO_{19}$ sample has a higher conductivity with increasing Zn-Mn doping mole fraction from 8.5 to 13.5 GHz. While the highest real sample permittivity is at the mole fraction x = 1 and the lowest is at x = 0. Overall the real value of permittivity has increased at a frequency of 10 to 14 GHz, where as for imaginary permittivity based on the mole fraction has increased permittivity, but has decreased with a frequency of 10 to 15 GHz. These results indicate that the $BaFe_{12-2x}Zn_x Mn_xO_{19}$ sample made from sand modified can application microwave absorber material at x-band frequency to Ku-band frequency.

ACKNOWLEDGMENTS

We wish to thank KEMENRISTEKDIKTI the financial support of this research, head of the analytical Chemistry Laboratory University of Mataram, LIPI laboratory, and all of who have contributed to this is research.

REFERENCES

1. Susilawati (2016). Synthesis and Characterization of Barium M-Hexaferrite With Mn and Ni Metal Doping for Microwaves. Green Development International Conference.
2. Feng Y.B., Qiu T., Shen C.Y., (2007), Journal of Magnetism and Magnetic Materials 318, 8 -13.
3. Ahmeda, Okashab, Kershi, (2008), Journal of Magnetism and Magnetic Materials 320, 1146–1150.
4. Susilawati, S., Doyan, A., Sahlam, S., and Pangga D. (2016). International Conference Theoretical and Application of Physics Journal.
5. Susilawati, S., Khairunnisa, K. and Doyan, A. (2015). Jurnal Pendidikan Fisika Dan Teknologi, 1(3).
6. Susilawati, Doyan, A., Taufik, M., Wahyudi, Ryantin G., E., Fitriani, A., Nazarudin. 2019. Journal Materials Science Forum, 966: 282-289.
7. Susilawati, Doyan, A., and M. Munib. (2015). Proceeding ICMSE ISBN 9786021570425.
8. Li, J., Zhang, H., Harris, V. G., Liao, Y., & Liu, Y. (2015). Journal of Alloys and Compounds, 649, 782-787.
9. Nuraini, U., Amalia, H., Rosyidah, K.C. and Zainuri, M. (2014). Crystal Structure and Magnetic Properties of Zn doped Barium M-Hexaferrite, 10(3)
10. Wagner, T.R. J. Solid State Chem. 136 (1998) 120–124.
11. Usvanda, L. N., & Zainuri, M. (2016). JurnalSains dan Seni ITS, 5(2).
12. Narang Bindra S. dan Hudiara I. S., (2006), Journal of Ceramic Processing Research., Vol. 7, No. 2, 113-116.
13. Sözeri, H., Deligöz, H., Kavas, H, and Baykal, A. (2014). Ceramics International, 40(6), 8645-8657 (2014).
14. Susilawati, Doyan, A., Khair, H., Taufik, M., Wahyudi. 2018. Journal of Physics: Conf. Series 1011 (2018) 012009.
15. Vázquez-Victorio, G. Flores-Martínez, N. Franceschin, G. Nowak, S. Ammar, S. Valenzuela, R. (2018). Journal of Superconductivity and Novel Magnetism. Vol. 31, issue 2, pp 347–351
16. Rahmawati, D. T., Kusumawati, D. H., & Rohmawati, L. (2015). Jurnal Fisika. Vol. 04 No. 01, 1-5.
17. Susilawati, Doyan, A., Khalilurrahman. 2017. AIP Conference Proceedings 1801, 040007. doi: org/10.1063/1.4973096.